ENSEMBLE DATA ASSIMILATION IN THE NCEP GFS

Jeffrey S. ***Whitaker*** [1] and *Thomas M.* ***Hamill*** [2]

NOAA CIRES Climate Diagnostics Center, Boulder, Colorado USA
[1] jeffrey.s.whitaker@noaa.gov and [2] tom.hamill@noaa.gov

1. Introduction

Ensemble-based data assimilation techniques (e.g. Houtekamer and Mitchell 1998, Hamill 2005) are now being actively explored as possible replacements for 3-dimensional or 4-dimensional variational analysis. With ensemble-based methods, parallel cycles of ensemble forecasts and updates to the observations are conducted; the ensemble of forecasts is used to estimate forecast-error statistics during the data assimilation step, and the output of the assimilation is a set of analyses, which are used as the initial conditions for the next ensemble of short-range forecasts.

Are ensemble data assimilation schemes competitive with operational NCEP 3D-Var method using realistic numer-ical weather prediction models and obser-vation data sets? Ideally, such a test would demonstrate the ability to assimilate the current full observational data set, including satellite radiances, using a high-resolution model and a large ensemble. However, computational expense of ensemble-based assimilation methods scale linearly with the number of observations, the number of ensemble members, and the dimension of the model state (Tippett et al. 2003), so a robust test like this is still not computationally feasible in a research environment. Accordingly, in this study we will explore ensemble-based data assimilation in a moderate-resolution general circulation model (GCM) assimilating a thinned set of observations. See also Houtekamer et al. (2005).

2. Model, observations, and data assimilation technique.

a. *Forecast Model.*

The forecast model is the NCEP Global Forecasting System (GFS) model, a global spectral model with a sigma vertical coordinate. We used the version of the model (wwwt.emc.ncep.noaa.gov/gmb/) operational in March 2004, but the resolution was reduced to T62 L28.

b. *Filter and computer configurations*.

The EnSRF is the data assimilation method used here. For brevity, a description of the method will be skipped. For details on this algorithm, see Whitaker and Hamill (2002). For a review of ensemble-based assimlation techniques in general, see Hamill (2005).

The EnSRF was run with 100 members. The analysis was performed on a 128*64 Gaussian grid at each of the 28 σ levels. The method was run on the NOAA High-Performance Computing System (http://hpcs.fsl.noaa.gov/) Intel Cluster.

The EnSRF used a horizontal covariance localization of the form in Gaspari and Cohn (1999), with the correlation function tapering to zero at 2800 km. A vertical localization was applied as well. For example, the increment from a surface observation tapered uniformly in σ to zero increment at 2 scale heights (that is, the σ such that $-\ln(\sigma) = 2$).

It was expected that the form of the model-error parameterization would have a substantial impact on the accuracy of the data assimilations. Here we will test three different approaches.

The first model error parameterization was covariance inflation (Anderson and Anderson 1999), which simply expands ensemble spread in the background's subspace. In this experiment, spreads were inflated by 30 % in the Northern Hemisphere (where observations are more plentiful, resulting in a smaller analysis spread), and 20 % in the Southern Hemisphere. The amount of inflation was tapered between the Northern

and Southern Hemispheric values between 25°N and 25°S. To make sure that spread was not inflated near the model top, where no observations make any increments, the inflation also was designed to taper to zero at six scale heights.

The second model-error parameterization was the Zhang et al. (2004) approach of relaxing the posterior back toward the prior. No noise is actually added to the background ensemble members, but after the update, the analysis perturbations are linearly combined with the background perturbations. The combination is 50/50.

The third approach was to add different random noise to each ensemble member. Here, the noise was generated from differences between random NCEP-NCAR reanalysis states separated by 6 h, scaled by 25 percent. Given that this experiment was conducted with January observational data, only reanalysis states from December, January, and February 1971-2000 were considered for random selection.

c. *Observations*.

Real observations were assimilated in this experiment. The observations consisted of NCEP's full quality controlled real-time data stream from January 2004, with the following exceptions. First, no satellite radiances or retrievals were assimilated; this left surface observations, raobs, cloud-drift winds, ACARS winds, and wind profilers. Due to problems in modeling the boundary layer, we chose to not assimilate observations below sigma level 0.9, with the exception of surface pressure, which was vertically adjusted to the model's orography. No humidity data was assimilated. This data amounted to approximately 145,000 observations at the 0000 and 1200 UTC, and 60,000 observations at the "off times" such as 1500 UTC.

Observation-error statistics were the same as those used operationally at NCEP in 2004. Observations were assimilated every 3 h. All observations were assumed to be valid at the time of the analysis; that is, in the data assimilation, the *H* operator does not interpolate between model forecast states to the time of the observations, as in "FGAT" (first guess at appropriate time) algorithms. An additional quality control "background" check to the observations was added. If the mean increment was too large, as measured by $\left|\mathbf{y} - H\overline{\mathbf{x}^b}\right| > 5(\sqrt{\mathbf{H}\mathbf{P}^b\mathbf{H}^{\mathrm{T}} + \mathbf{R}}$, then the observation was not assimilated. Here, $\mathbf{P}^b$ and $\mathbf{R}$ denote the background-error and the observation-error covariance matrices, respectively. **H** is a linearization of *H*, the observation operator, converting the model state to the observation location and type, **y** is the observation vector, and $\overline{\mathbf{x}^b}$ is the ensemble mean background.

3. **Results**.

Figure 1 shows the time-averaged spread in the random noise model error simulation before and after the introduction of the model error. Note that noise was preferentially introduced in the storm tracks. It was not apparent whether a priori whether this was desirable.

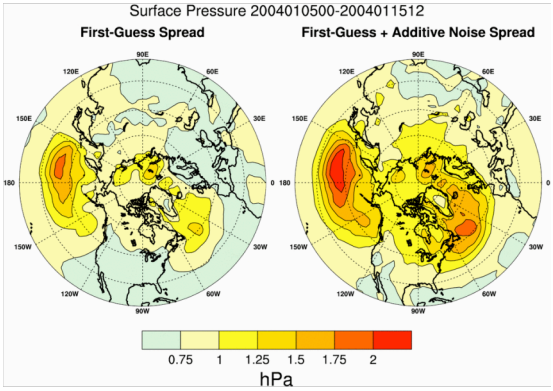

Figure 1: Time-averaged surface-pressure spread (hPa) before and after additive model errors were added to background ensemble.

For the random additive error run, the Northern Hemispheric spread of surface pressure in the analysis was 0.707 hPa. For the background forecast 3 h later, before the introduction of random noise, the spread was 0.932 hPa. After the introduction of random noise to simulate model error, the spread was increased to 1.044 hPa. The most apparent thing from these statistics is the relatively rapid growth of errors in the 3 h subsequent to the forecast. For comparison, the observation-error spread statistic for surface pressure were 1.0 hPa over land and 1.6 hPa over water.

3-day forecast errors from a variety of analyses are shown in Fig. 2. These statistics reflect the errors for a 10-day period in January after a 5-day spinup. The T62 forecast errors from the EnSRF with the three different model error parameterizations are shown, as well as forecasts from the NCEP-NCAR reanalysis 2 (R2), and forecasts initialized with the operational T255 GDAS ("Global Data Assimilation System," a spectral-statistical interpolation 3D-Var technique based on Parrish and Derber 1992). R2 used a somewhat different data set, including satellite retrieval information, but the reanalysis was cycled forward with an older, 1998 version of the GFS. The operational T255 GDAS included a large number of satellite radiances that were not assimilated in any of the square-root filter implementations.

Figure 2 shows that the smallest meridional wind forecast error relative to the assumed truth, the GDAS, was forecasts initialized with the GDAS itself. Somewhat larger errors occurred in forecasts initialized from the additive error EnSRF and R2, with the EnSRF slightly smaller in error. The covariance inflation EnSRF and Zhang et al. approach were somewhat worse. The differences in these forecasts were somewhat subtle. For example, the reduction in error between GDAS and the additive-error EnSRF amounted to about a 3-6 hour extension in forecast lead time.

Is there any reason to expect that the flow-dependent error covariances provided any beneficial influence in the data assimilation? Figure 3 indicates that there may be some benefit. Here the EnSRF algorithm was re-run, but at each assimilation time the flow-dependent perturbations were totally replaced by random "model errors." As can be seen, the EnSRF where some model error was added to forecasts was significantly smaller in error than the EnSRF with the total replacement of perturbations.

Still, why weren't the ensemble filters performing more skillfully than the existing 3D-Var from GDAS? In a previous experiment with a sparse network of surface-pressure observations, the ensemble filter outperformed 3D-Var (Whitaker et al. 2004). However, the potential advantage offered by ensemble-based data assimilation methods, improved background-error covariances, is less crucial to data assimilation accuracy when observations are plentiful. Hence, the result is perhaps not so surprising, for GDAS used many more observations. Another possible advantage is that the GDAS was conducted with a much higher resolution forecast/analysis system (T255).

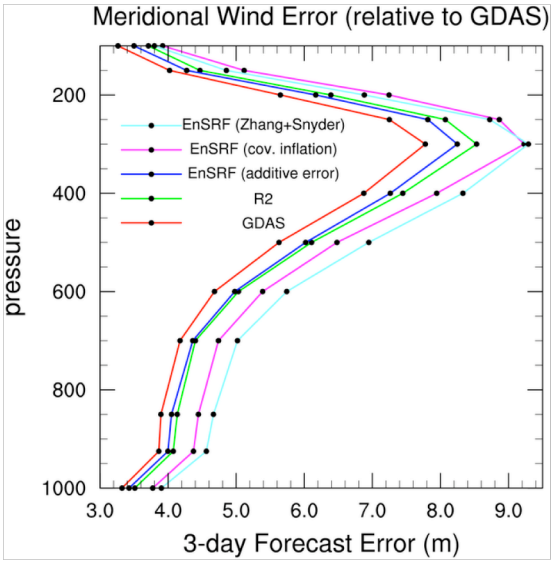

Figure 2: Time-averaged 72-h meridional wind forecast errors initialized from the different data assimilation methods.

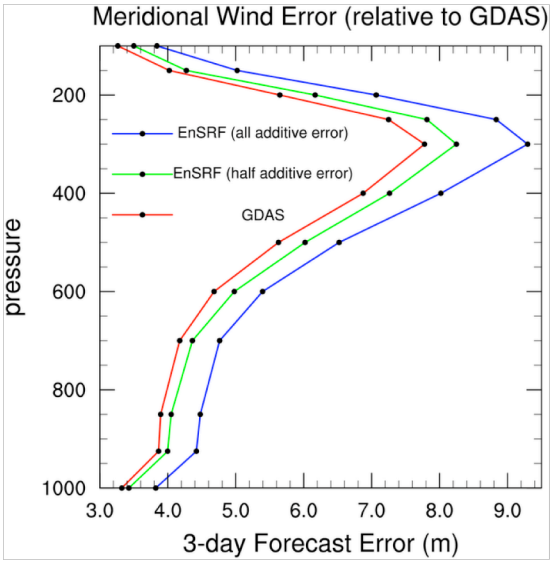

Figure 3. 72-h forecast errors from the GDAS, EnSRF, and filter where flow-dependent perturbations were replaced with additive errors.

The most appropriate benchmark would be forecasts from the operational GDAS at T62 resolution assimilating the same subset of observations as the ensemble filters assimilated. Unfortunately, these results were not available at the time of preparation of this manuscript. We are working with staff at NCEP to generate these analyses and forecasts.

4. **Conclusions**

A 100-member ensemble-based data assimilation method was tested in a T62 GCM with a somewhat reduced set of observations (primarily no satellite radiances). The ensemble method, the EnSRF, produced analyses that were competitive in quality to the NCEP-NCAR reanalysis, which assimilated more observations but used an older version of the forecast model.

These results suggest the potential operational utility of ensemble-based data assimilation methods. There are still some important questions to address, including how error characteristics might be improved (observation and model error), the importance of resolution (would a higher-resolution model produce more realistic background forecasts?) and the computational expense (can an algorithm be designed whose costs do not scale linearly with the number of observations?).

Acknowledgments: This research was supported by a NOAA THORPEX grant.

References

Anderson, J. L., and S. L. Anderson, 1999: A Monte Carlo implementation of the nonlinear filtering problem to produce ensemble assimilations and forecasts. *Mon. Wea. Rev.*, **127**, 2741-2758.

Gaspari, G. and S. E. Cohn, 1999: Construction of correlation functions in two and three dimensions. *Quart. J. Royal Meteor. Soc.*, **125**, 723-757.

Hamill, T. M., 2005: Ensemble-based atmospheric data assimilation. To appear in *Predictability of Weather and Climate*, T. N. Palmer and R. Hagedorn, eds. Cambridge Press. Available at www.cdc.noaa.gov/people/tom.hamill/efda_review5.pdf .

Houtekamer, P. L., and H. L. Mitchell, 1998: Data assimilation using an ensemble Kalman filter technique. *Mon. Wea. Rev.*, **126**, 796-811.

----------, ----------, G. Pellerin, M. Buehner, M. Charron, L. Spacek, and B. Hansen, 2004: Atmospheric data assimilation with the ensemble Kalman filter: results with real observations. *Mon. Wea. Rev.*, in press.

Parrish, D. F., and J. C. Derber, 1992: The National Meteorological Center's Spectral Statistical Interpolation Analysis System. *Mon. Wea. Rev.*, **120**, 1747-1763.

Tippett, M. K., J. L. Anderson, C. H. Bishop, T. M. Hamill, and J. S. Whitaker, 2003: Ensemble square root filters. *Mon. Wea. Rev.*, **131**, 1485-1490.

Whitaker, J. S., and T. M. Hamill, 2002: Ensemble data assimilation without perturbed observations. *Mon. Wea. Rev.*, **130**, 1913-1924.

----------, G. P. Compo, X. Wei, and T. M. Hamill, 2004: Reanalysis without radiosondes using ensemble data assimilation. *Mon. Wea. Rev.*, **132,** 1190-1200.

Zhang, F., C. Snyder, and J. Sun, 2004: Impacts of initial estimate and observation availability on convective-scale data assimilation with an ensemble Kalman filter. *Mon. Wea. Rev.*, **132**, 1238-1253.